THEORETICAL ELUCIDATION OF THE UNUSUALLY HIGH [HNC]/[HCN] ABUNDANCE RATIO IN INTERSTELLAR SPACE: TWO-DIMENSIONAL AND TWO-STATE QUANTUM WAVE PACKET DYNAMICS STUDY ON THE BRANCHING RATIO OF THE DISSOCIATIVE RECOMBINATION REACTION $HCNH^+ + e^- \rightarrow HNC/HCN + H$

KEISAKU ISHII,[1] ASAMI TAJIMA,[2] TETSUYA TAKETSUGU,[3] AND KOICHI YAMASHITA[1]

ABSTRACT

In order to elucidate the unusually high [HNC]/[HCN] abundance ratio observed in interstellar space, we have carried out wave packet simulations for the dissociative recombination reaction $HCNH^+ + e^- \rightarrow HNC/HCN + H$ on the two-dimensional potential energy surfaces (PESs) of two dissociative electronic states of HCNH, $1\,^2\Sigma^+$ and $2\,^2\Sigma^+$. Two adiabatic PESs of $1\,^2\Sigma^+$ and $2\,^2\Sigma^+$ have been determined as functions of NH and CH bond lengths for a linear geometry of HCNH with a fixed CN bond length, by the multireference single and double configuration interaction plus Davidson's quadruple excitation correction [MR-SDCI(+Q)] method. The wave packets, generated from the low-lying vibrational eigenstates of $HCNH^+$, have been put initially on the $2\,^2\Sigma^+$ adiabatic PES. The resulting branching ratios of [HNC]/[HCN] vary from 0.77 to 1.32, depending on the initial vibrational quantum numbers, which support that $HCNH^+$ is the precursor of both HNC and HCN in interstellar space.

Subject headings: astrochemistry — ISM: molecules — molecular processes

1. INTRODUCTION

Highly accurate ab initio molecular orbital (MO) calculations by the coupled cluster [CCSD(T)] method showed (Bowman et al. 1993) that HNC is less stable than HCN by 0.62 eV. This means that there should be almost no abundance of HNC compared with HCN in a thermochemically equilibrated system at low temperature, like interstellar space. Contradicting this thermochemical consideration, however, the abundance ratios of [HNC]/[HCN] are observed to be on the order of 1 to 1/100 in many interstellar spaces (Wooten et al. 1978; Irvine et al. 1987; Schilke et al. 1992; Hirota et al. 1998). Ratios are generally high in dark cloud cores, i.e., 4.4 in L134 (Wooten et al. 1978), 4.5 in L1498, and 0.45 in L1521E with an average value of 2.1 (Hirota et al. 1998), and low (1 to 1/90) in high kinetic temperature regions such as the OMC-1 hot core (Schilke et al. 1992). One of the astrochemical hypotheses that explains such an unusually high HNC abundance in interstellar clouds is that $HCNH^+$ is the precursor of both HNC and HCN, and the dissociative recombination (DR) reaction with an electron,

$$HCNH^+ + e^- \rightarrow HNC/HCN + H, \qquad (1)$$
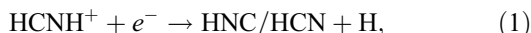
is postulated to be the main process for the production of both HNC and HCN (Watson 1974). The HNC/HCN branching ratio has been thought to be almost 1. Herbst (1978) predicted, using statistical phase-space theory, that three products, HNC, HCN, and CN, are formed with the ratio of 1:1:2 in the $HCNH^+ + e^-$ DR reaction. Barger et al. (2003) studied radiative relaxation and isomeric branching of the highly excited H/C/N system, which

might be produced from the DR reaction (1), and found that the radiative branching between the isomers is highly dependent on the identity of the initial vibrational state. The HCN-local and HNC-local vibrational states radiate within the respective structures, while delocalized states above the barrier of the HNC/HCN isomerization reaction (1.89 eV from the HCN side and 1.26 eV from the HNC side; Bowman et al. 1993) relax radiatively to both isomers.

$HCNH^+$ was first identified in the laboratory by Altman et al. (1984a, 1984b) by infrared spectroscopy, and later pure rotational spectroscopy was reported by Bogey et al. (1985). In 1986 $HCNH^+$ was detected in interstellar space toward Sgr B2 by Ziurys & Turner (1986). Recently, Semaniak et al. (2001) studied the DR of $HCNH^+ + e^-$ with a heavy-ion storage ring and measured branching fractions for different dissociation channels at a collision energy of 0 eV: HCN(HNC) + H (0.67), $CN + H_2$ (0), and $CN + H + H$ (0.33). This result indicates that the DR of $HCNH^+$ is an efficient process leading to the formation of HNC/HCN isomers, but the branching ratio of HNC/HCN was not resolved.

To elucidate details of the DR process, it is indispensable to investigate features of the relevant potential energy surfaces (PESs) with theoretical calculations. One of the present authors (K. I.) and coworkers (Shiba et al. 1998) carried out ab initio MO calculations for electronic excited states of HCNH, leading to the proposal of an indirect mechanism for the DR reaction of $HCNH^+ + e^-$. Below the ground state of $HCNH^+$ there are only three valence electronic states of the neutral HCNH, i.e., $1\,^2\Pi$, $1\,^2\Sigma^+$, and $2\,^2\Sigma^+$, the latter two of which are dissociative with respect to CH and NH bond cleavages. The dissociative PESs of these $1\,^2\Sigma^+$ and $2\,^2\Sigma^+$ states show an avoided crossing feature with each other around the equilibrium structure of $HCNH^+$. There is no crossing between the dissociative states of HCNH and the ground state of $HCNH^+$ near the equilibrium structure of $HCNH^+$, and thus we proposed the indirect mechanism for this DR reaction. Talbi and coworkers, however, proposed the direct mechanism based on the results of their ab initio MO calculations (Talbi & Ellinger 1998; Hickman et al. 2005). Very recently, we carried out ab initio direct trajectory simulations (Taketsugu et al. 2004)

[1] Department of Chemical System Engineering, School of Engineering, The University of Tokyo, Tokyo 113-8656, Japan; ishii@tcl.t.u-tokyo.ac.jp, yamasita@chemsys.t.u-tokyo.ac.jp.

[2] Department of Chemistry, Faculty of Science, Ochanomizu University, Tokyo 112-8610, Japan; asami@chem.ocha.ac.jp.

[3] Division of Chemistry, Graduate School of Science, Hokkaido University, Sapporo 060-0810, Japan; take@sci.hokudai.ac.jp.

for reaction (1), taking into account nonadiabatic transitions among adiabatic electronic states, and showed that among 50 trajectories, 24 lead to HNC + H, 21 lead to HCN + H, three lead to CN + H + H, and two remain in the region of HCNH. This result also supports that HNC and HCN are generated with almost the same amount from reaction (1).

In the ab initio direct trajectory simulations, nuclear motions were followed by the classical Newton equation of motion. In this study, we carry out quantum wave packet simulations for reaction (1) within the two-dimensional reduced coordinate space on the PESs obtained by highly correlated ab initio MO calculations and discuss the branching ratio of [HNC]/[HCN] through quantum mechanical simulations.

2. METHODS OF CALCULATIONS

In the present simulation three assumptions have been applied: (1) The series of Rydberg states converging upward to the ground state of the $HCNH^+$ cation has been neglected, because the PESs of Rydberg states are parallel to the PES of the ground state of $HCNH^+$ and are not dissociative in the diabatic picture. (2) The linear geometry is assumed because of the stability of linear geometry in the significant electronic states, $X\,^1\Sigma^+$ of $HCNH^+$ and $1\,^2\Sigma^+$ and $2\,^2\Sigma^+$ of neutral HCNH. (3) The $1\,^2\Pi$ state of HCNH was neglected, because Σ and Π states do not interact with each other in the linear geometry.

Ab initio calculations were carried out for the $X\,^1\Sigma^+$ state of $HCNH^+$ and the $1\,^2\Pi$, $1\,^2\Sigma^+$, and $2\,^2\Sigma^+$ states of neutral HCNH in the linear geometry by the complete active space self-consistent field (CASSCF; Werner & Knowles 1985) and the multireference single and double configuration interaction method (Werner & Knowles 1988) plus corrections for Davidson's quadruple excitations [MR-SDCI(+Q)] with the correlation consistent polarized valence quadruple zeta basis sets (cc-pVQZ; Dunning 1989), using the MOLPRO program package.[4] These ab initio methods are almost the same as those of the previous study (Shiba et al. 1998), although Davidson's corrections were not included previously. Adiabatic energies were calculated at 441 points in the regions of $r(\mathrm{CH}) \simeq 0.7\text{--}2.7$ Å and $r(\mathrm{NH}) \simeq 0.7\text{--}2.7$ Å, and the energies in the region outside of $r > 2.7$ Å were set to the same values at $r = 2.7$ Å, where the CN bond length was fixed at the equilibrium bond length in $HCNH^+$ (1.139 Å). The thus obtained adiabatic energies of the $1\,^2\Sigma^+$ and $2\,^2\Sigma^+$ states were diabatized by using the dipole moment matrices (Werner & Meyer 1981), whose diagonal elements are the dipole moments of the $1\,^2\Sigma^+$ and $2\,^2\Sigma^+$ states and whose off-diagonal elements are transition dipole moments between the two adiabatic $^2\Sigma^+$ states. The diabatized $^2\Sigma^+$ states are dissociative with respect to either the NH bond [$^2\Sigma^+(\sigma^*(\mathrm{NH}))$] or CH bond [$^2\Sigma^+(\sigma^*(\mathrm{CH}))$]. The calculated adiabatic and diabatic potential energies were fitted, respectively, to the spline functions.

In the wave packet simulations, we employed the grid-based method developed by Kosloff (1988). The two-dimensional coordinate space was represented by a uniform 256×256 grid. Figure 1 shows the definition of coordinates r_1 and r_2, which are distances of the respective H atoms from the center of mass of the CN fragment. The time-dependent Schrödinger equation for
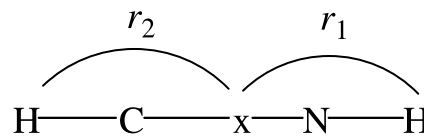
Fig. 1.—Definition of coordinates r_1 and r_2.

the two $^2\Sigma^+$ states in the diabatic representation can be written as

$$i\hbar \frac{\partial}{\partial t}\begin{pmatrix} \Psi_1(r_1, r_2, t) \\ \Psi_2(r_1, r_2, t) \end{pmatrix}$$
$$= \begin{pmatrix} H_{11}(r_1, r_2) & V_{12}(r_1, r_2) \\ V_{12}(r_1, r_2) & H_{22}(r_1, r_2) \end{pmatrix}\begin{pmatrix} \Psi_1(r_1, r_2, t) \\ \Psi_2(r_1, r_2, t) \end{pmatrix}, \quad (2)$$

where Ψ_1 and Ψ_2 are the nuclear wave functions for the $^2\Sigma^+(\sigma^*(\mathrm{NH}))$ and $^2\Sigma^+(\sigma^*(\mathrm{CH}))$ dissociative states, respectively, H_{11} and H_{22} are the diagonal terms of the Hamiltonian matrix, and V_{12} is the diabatic coupling potential between the two $^2\Sigma^+$ states. Here H_{11} and H_{22} are expressed as

$$H_{11}(r_1, r_2) = T(r_1, r_2) + V_{11}(r_1, r_2) + V_{\mathrm{eff}}(r_1, r_2), \quad (3)$$

$$H_{22}(r_1, r_2) = T(r_1, r_2) + V_{22}(r_1, r_2) + V_{\mathrm{eff}}(r_1, r_2), \quad (4)$$

where

$$T(r_1, r_2) = -\frac{\hbar^2}{2\mu}\frac{\partial^2}{\partial r_1^2} - \frac{\hbar^2}{2\mu}\frac{\partial^2}{\partial r_2^2}, \quad (5)$$

$$V_{\mathrm{eff}}(r_1, r_2) = -\frac{\hbar^2}{8}\left(\frac{1}{\mu r_1^2} + \frac{1}{\mu r_2^2}\right), \quad (6)$$

$$\frac{1}{\mu} = \frac{1}{m_\mathrm{H}} + \frac{1}{m_\mathrm{H} + m_\mathrm{C} + m_\mathrm{N}}, \quad (7)$$

and V_{11} and V_{22} are the diabatic potential energies for $^2\Sigma^+(\sigma^*(\mathrm{NH}))$ and $^2\Sigma^+(\sigma^*(\mathrm{CN}))$, respectively. The kinetic energy operator T, the effective potential V_{eff}, and the reduced mass μ are derived from the Hamiltonian for acetylene (Bentley et al. 1992). It is noted that rotational degrees of freedom of nuclear motions were ignored in the present simulation.

In the indirect process of the DR reaction, the molecule will acquire the kinetic energy while descending the dense manifold of Rydberg states, which transforms to the vibrational energy. When attaining the $2\,^2\Sigma^+$ valence electronic state, the molecular state will be written as a linear combination of the vibrational eigenstates of $HCNH^+$ approximately. To prepare the initial wave packets, we applied the relaxation method (Kosloff & Tal-Ezer 1986) to generate six low-lying vibrational eigenstates, $(v_1, v_2) = (0, 0), (0, 1), (1, 0), (0, 2), (1, 1),$ and $(2, 0)$, where v_1 and v_2 denote quantum numbers for NH and CH stretching vibrational modes of the $HCNH^+$ cation, respectively. Those wave packets were put on the neutral adiabatic $2\,^2\Sigma^+$ state in the Franck-Condon way and were propagated for 80 fs with a fixed time step of 0.1 a.u. by the second-order differentiation method (Askar & Cakmak 1978). The wave functions in the adiabatic representation can be calculated by the reverse unitary transformation from the diabatic wave functions. The branching ratio of [HNC]/[HCN] was
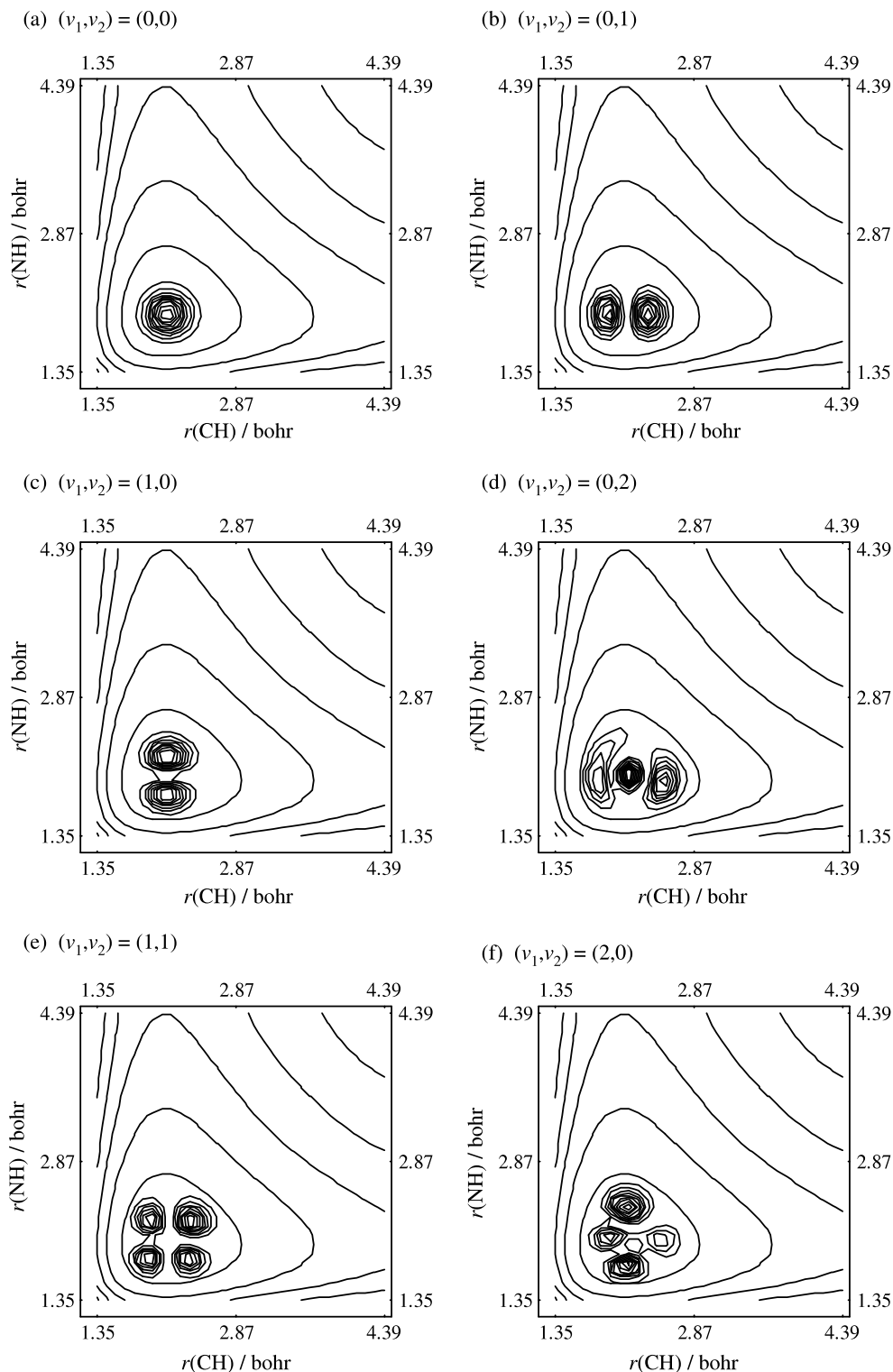
FIG. 2.—Vibrational eigenstates of HCNH$^+$ with vibrational quantum numbers (a) $(v_1, v_2) = (0,0)$, (b) $(0, 1)$, (c) $(1, 0)$, (d) $(0, 2)$, (e) $(1, 1)$, and (f) $(2, 0)$.

estimated from the ratio of norms of wave functions, $|\Psi_2|^2/|\Psi_1|^2$, in the regions of $r(\text{NH}) > 3.25$ bohr or $r(\text{CH}) > 3.25$ bohr.

3. RESULTS AND DISCUSSION

The energy difference between the $X\,^1\Sigma^+$ state of HCNH$^+$ and the $2\,^2\Sigma^+$ state of neutral HCNH at the cation equilibrium structure was evaluated as 1.68 eV (13400 cm^{-1}; Shiba et al. 1998). Upon the catch of an electron by HCNH$^+$, this excess electronic energy may be redistributed to vibrational modes during relaxation through the dense manifold of Rydberg states, and thus the nuclear wave function can be expressed as a linear combination of different vibrational eigenstates of various Rydberg electronic states. Figure 2 shows vibrational eigenstates of HCNH$^+$, specified by vibrational quantum numbers $(v_1, v_2) = (0, 0)$, $(0, 1)$, $(1, 0)$, $(0, 2)$, $(1, 1)$, and $(2, 0)$, the energies of which were evaluated as 0, 3069, 3320, 6146, 6389, and 6470 cm^{-1}, respectively.
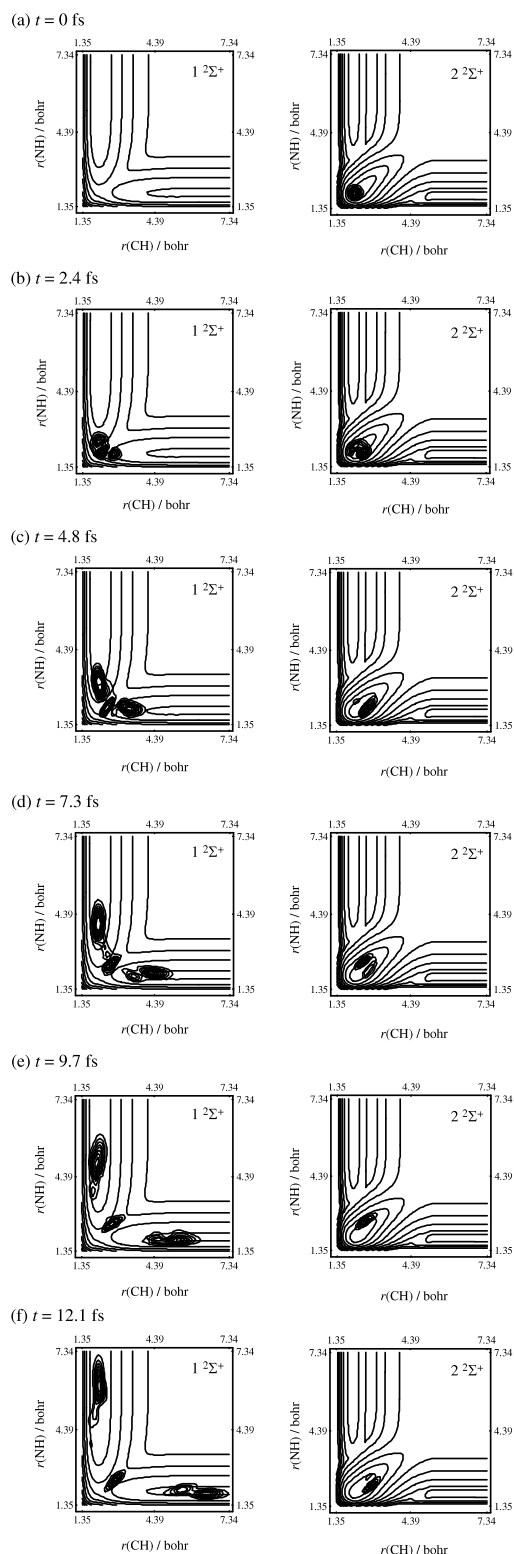
(a) $t = 0$ fs

(b) $t = 2.4$ fs

(c) $t = 4.8$ fs

(d) $t = 7.3$ fs

(e) $t = 9.7$ fs

(f) $t = 12.1$ fs

Fig. 3.—Time propagation of the wave packets on the $1\,{}^2\Sigma^+$ and $2\,{}^2\Sigma^+$ states: (a) $t = 0$, (b) $t = 2.4$ fs, (c) $t = 4.8$ fs, (d) $t = 7.3$ fs, (e) $t = 9.7$ fs, and (f) $t = 12.1$ fs.

Fig. 4.—Variations of norms of the adiabatic states for the wave packet starting from $(v_1, v_2) = (0, 0)$.

The experimental energy levels (fundamental frequencies) were reported as 3187.9 and 3482.8 cm^{-1} for the (0, 1) and (1, 0) states, respectively (Altman et al. 1984a, 1984b).

Figure 3 shows the time propagation of the wave packet, starting from the (0, 0) eigenstate, in the adiabatic representation. Initially the wave packet is located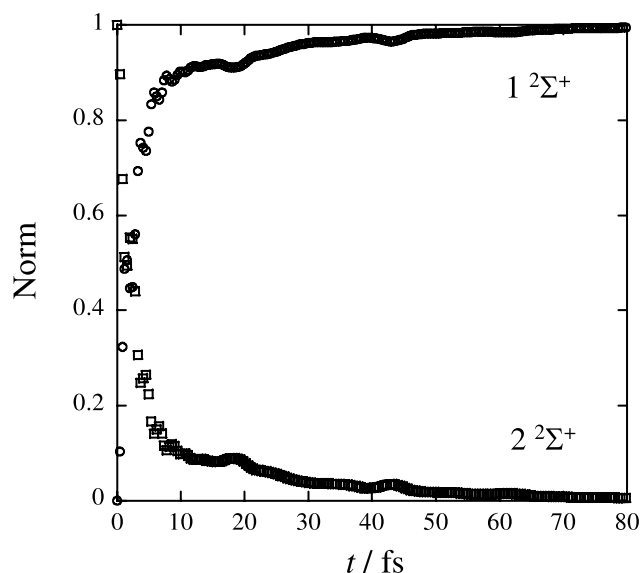 only on the $2\,{}^2\Sigma^+$ state, and there is no population on the $1\,{}^2\Sigma^+$ state (Fig. 3a). At $t = 2.4$ fs a large amount of the wave packet makes the nonadiabatic transition from $2\,{}^2\Sigma^+$ to $1\,{}^2\Sigma^+$, and the wave packet in $1\,{}^2\Sigma^+$ begins to divide into three portions (Fig. 3b). At $t = 4.8$ and 7.3 fs the wave packet in $1\,{}^2\Sigma^+$ splits into three portions clearly, where the first fragment is going to the HCN + H channel, the second is going to the HNC + H channel, and the third remains in the Franck-Condon region (Figs. 3c and 3d). At $t = 9.7$ and 12.1 fs the wave packet in $1\,{}^2\Sigma^+$ is completely separated into three portions (Figs. 3e and 3f).

Figure 4 shows the variation of the norm of the wave packets in the adiabatic representation. Initially the populations for $1\,{}^2\Sigma^+$ and $2\,{}^2\Sigma^+$ states are 0 and 1, respectively. At $t = 2.7$ fs 50% of the wave packet makes the nonadiabatic transition from $2\,{}^2\Sigma^+$ to $1\,{}^2\Sigma^+$, resulting in norms of 0.5 for both $1\,{}^2\Sigma^+$ and $2\,{}^2\Sigma^+$ states. At $t = 10$ fs 90% of the wave packet has been transferred from $2\,{}^2\Sigma^+$ to $1\,{}^2\Sigma^+$, and at $t = 80$ fs only 1% of the wave packet remains on the $2\,{}^2\Sigma^+$ PES. In previous ab initio direct trajectory simulations (Taketsugu et al. 2004), the surface hopping from $2\,{}^2\Sigma^+$ to $1\,{}^2\Sigma^+$ occurred within 5 fs in 34% of trajectories, and this rate increased to 76% at $t = 10$ fs. In both quantum and semiclassical simulations, the initial transition from $2\,{}^2\Sigma^+$ to $1\,{}^2\Sigma^+$ states occurs very quickly, indicating the strong coupling of these two adiabatic states in the Franck-Condon region just below the equilibrium structure of the cationic ground state.

In the present wave packet simulations, the branching ratio of [HNC]/[HCN] is calculated as 0.77 for the case starting with $(v_1, v_2) = (0, 0)$. The wave packets starting with other initial vibrational states have shown similar behaviors. The final branching ratios are listed in Table 1: 0.77 for (0, 0), 1.32 for (0, 1), 0.79 for (1, 0), 1.13 for (0, 2), 0.96 for (1, 1), and 1.00 for (2, 0). It is noted that in ab initio direct trajectory simulations where zero-point vibrational energies were given to the respective vibrational modes in the initial states, the branching ratio of [HNC]/[HCN] was evaluated as 1.14 (Taketsugu et al. 2004). We should also pay attention to the radiative relaxation study of the highly excited H/C/N system (Barger et al. 2003), in which the radiative branching ratio of HNC/HCN was shown to be on the order of 1 when highly excited delocalized states above the barrier to isomerization are included in the initial states. These results indicate that the branching ratio of [HNC]/[HCN] for the DR

TABLE 1

Branching Ratios of [HNC]/[HCN] for the HCNH$^+$ + e^- Reaction, Starting with Different Vibrational Quantum Numbers (v_1, v_2)

(v_1, v_2)	[HNC]/[HCN]
(0, 0)..	0.77
(0, 1)..	1.32
(1, 0)..	0.79
(0, 2)..	1.13
(1, 1)..	0.96
(2, 0)..	1.00

reaction (1) is on the order of 1, even when the excess electronic energy between the $X\ ^1\Sigma^+$ state of HCNH$^+$ and 2 $^2\Sigma^+$ state of HCNH has been completely redistributed to the internal energy of the product HCN or HNC.

As described in the introduction, Talbi and coworkers (Talbi & Ellinger 1998; Hickman et al. 2005) proposed the direct mechanism for the DR reaction of HCNH$^+$. In the latest paper (Hickman et al. 2005), they insist that our previous calculations (Shiba et al. 1998) are insufficient because of the lack of Rydberg orbitals in the atomic basis sets and that the two lowest HCNH $^2\Sigma^+$ dissociative states should cross the PES of the cation. This statement is, however, not true. The inclusion of Rydberg orbitals means an increase of variational parameters, and this does not cause a rise in the energies because of the variational principle. Therefore, the two lowest HCNH $^2\Sigma^+$ dissociative states do not cross the PES of HCNH$^+$ even if we add Rydberg orbitals to the basis sets.

Finally, we provide comments on the assumptions of the linear geometry. Due to this restriction, HCNH bending motions and isomerization reactions between HNC and HCN have not been permitted. According to ab initio direct trajectory simulations (Taketsugu et al. 2004), actually the molecule begins to bend in the nonadiabatic region between 1 $^2\Pi$ and 1 $^2\Sigma^+$, and the isomerization reactions between HNC and HCN occur in three cases among 50 trajectories during the dissociation processes. This amount is small but not negligible, and thus we plan to investigate the effects of bending motions on the branching ratios by performing four-dimensional three-state quantum wave packet simulations. Such simulations can evaluate the branching ratios of the other products, CN + H + H, which were reported as about 30% by Semaniak et al. (2001).

4. CONCLUDING REMARKS

In this paper the branching ratio of the DR of HCNH$^+$ + e^- has been studied by quantum wave packet simulations on the PESs obtained by highly correlated ab initio MO methods. The resulting branching ratios of [HNC]/[HCN] vary from 0.77 to 1.32 with different vibrational quantum numbers of the initial wave packets. These consequences agree well with those of our recent ab initio surface-hopping trajectory simulations (Taketsugu et al. 2004), which include the 1 $^2\Pi$ electronic state and H-C-N-H bending motions. Now the branching ratio of reaction (1) is shown to be on the order of 1, and the astrochemical hypothesis that both HNC and HCN are produced by the DR of HCNH$^+$ and that the branching ratio is nearly 1 has been confirmed by the quantum mechanical simulations.

REFERENCES

Altman, R. S., Crofton, M. W., & Oka, T. 1984a, J. Chem. Phys., 80, 3911
———. 1984b, J. Chem. Phys., 81, 4255
Askar, A., & Cakmak, A. S. 1978, J. Chem. Phys., 68, 2794
Barger, T., Wodtke, A. M., & Bowman, J. M. 2003, ApJ, 587, 841
Bentley, J. A., Wyatt, R. E., Menou, M., & Leforestier, C. 1992, J. Chem. Phys., 97, 4255
Bogey, M., Demuynck, C., & Destombes, J. L. 1985, J. Chem. Phys., 83, 3703
Bowman, J. M., Gazdy, B., Bentley, J. A., Lee, T. J., & Dateo, C. E. J. 1993, J. Chem. Phys., 99, 308
Dunning, T. H., Jr. 1989, J. Chem. Phys., 90, 1007
Herbst, E. 1978, ApJ, 222, 508
Hickman, A. P., Miles, R. D., Hayden, C., & Talbi, D. 2005, A&A, 438, 31
Hirota, T., Yamamoto, S., Mikami, H., & Ohishi, M. 1998, ApJ, 503, 717
Irvine, W. M., Goldsmith, P. F., & Hjalmarson, Å. 1987, in Interstellar Process, ed. D. J. Hollenbach & H. A. Thronson, Jr. (Dordrecht: Reidel), 561

Kosloff, R. 1988, J. Phys. Chem., 92, 2087
Kosloff, R., & Tal-Ezer, H. A. 1986, Chem. Phys. Lett., 127, 223
Schilke, P., Walmsley, C. M., Pineau des Forêts, G., Roueff, E., Flower, D. R., & Guilloteau, S. 1992, A&A, 256, 595
Semaniak, J., et al. 2001, ApJS, 135, 275
Shiba, Y., Hirano, T., Nagashima, U., & Ishii, K. 1998, J. Chem. Phys., 108, 698
Taketsugu, T., Tajima, A., Ishii, K., & Hirano, T. 2004, ApJ, 608, 323
Talbi, D., & Ellinger, Y. 1998, Chem. Phys. Lett., 288, 155
Watson, W. D. 1974, ApJ, 188, 35
Werner, H.-J., & Knowles, P. J. 1985, J. Chem. Phys., 82, 5053
———. 1988, J. Chem. Phys., 89, 5803
Werner, H.-J., & Meyer, W. 1981, J. Chem. Phys., 74, 5802
Wooten, A., Evans, N. J., II, Snell, R., & Bout, P. V. 1978, ApJ, 225, L143
Ziurys, L. M., & Turner, B. E. 1986, ApJ, 302, L31